A new, versatile, direct-current helium atmospheric-pressure glow discharge

Francisco J. Andrade,* William C. Wetzel, George C.-Y. Chan, Michael R. Webb, Gerardo Gamez, Steven J. Ray and Gary M. Hieftje

Received 30th May 2006, Accepted 19th September 2006
First published as an Advance Article on the web 5th October 2006
DOI: 10.1039/b607544d

A novel direct current glow discharge sustained in helium at atmospheric pressure has been developed. Current–voltage behavior and spectroscopic characteristics strongly suggest that the system operates in the glow regime, in spite of the high pressure. The diffuse and extremely stable discharge is typically operated within a voltage range of 300–900 volts (in the current-controlled mode) and at currents ranging over tens to hundreds of milliamps. Spatially resolved spectroscopic measurements of some selected species are presented. Rotational temperature profiles were calculated using the OH emission spectrum, yielding values in the positive column ranging from 1300 to 1600 K.

Introduction

Glow discharges (GD) have become invaluable analytical sources for both optical and mass spectrometry.[1] Though their analytical application has been traditionally focused on the elemental characterization of solid samples, suitable schemes for the analysis of gases[2] and liquids[3] have also been developed. Direct current (dc) GDs allow the analysis of conductive materials, while radiofrequency powering schemes must typically be used for non-conductive samples. For both powering methods, depth-resolved elemental profiles can be obtained. New areas of application, such as the use of GDs for the ionization of organic compounds, have also been explored. In this case, it has been shown that by pulsing[4–6] the GD, switching the polarity of the electrodes,[7] or implementing a flowing afterglow technique,[8,9] information at both the elemental and molecular levels can be generated. Overall, few sources display the versatility and simplicity of GDs, which makes them extremely powerful tools for facing new challenges in chemical analysis.[10]

In spite of these advantages, the operating pressure of GDs, typically in the single Torr range, sometimes limits their performance. At reduced pressure, sample introduction becomes more complex and special arrangements, such as atmospheric-sampling devices,[2] have been developed to partially overcome this problem. Desolvation in a low-pressure GD is inefficient, so liquid samples must usually be dried before being introduced into the discharge cell.[3] Also, the necessity of working at reduced pressure can increase instrumental complexity. In fast-flowing afterglow strategies, for example, the use of a high gas flow requires a significant pumping capacity.[11] Additional limitations arise when GDs are used for the ionization of organic compounds. At reduced pressure, molecules generally undergo minimal collisional relaxation, which favors fragmentation. Thus, obtaining intact parent molecular ions with a GD becomes more difficult, and often requires a pulsed powering scheme and time-resolved detection.[6,12] For these reasons, there has long been an interest in developing GDs that can be operated at atmospheric pressure.

One limitation to operating direct-current GDs at higher pressures lies in the glow-to-arc transition (GAT). Elevating the pressure favours the onset of instabilities on the surface of the electrodes which, in a direct current GD, will ultimately lead to an arc.[13–15] Glow discharges and arcs represent two significantly different regimes. GDs are stable, diffuse, high-voltage and low-current sources: each of these characteristics is intimately related to the analytical performance of the GD. High voltages provide electrons with considerable energy from the applied electrical field, which is then transmitted to other species without extensive heating of the gas. Arcs, on the other hand, are sustained with low voltages and high currents, resulting in high gas temperatures. This thermal process generates density gradients in the gas, which lead to a filamentary and typically unstable discharge. For these reasons, avoiding the GAT is extremely important in order to preserve the desirable analytical features of GDs.

Efforts to develop GDs that can be sustained at atmospheric pressure have been focused on minimizing the effect of transient instabilities of the electrical field on the surface of the electrodes, either by changing the system geometry or by using alternative powering schemes. Changes to the system geometry are based on similarity laws, which state that the gap between the electrodes must be reduced as the pressure is raised, in order to maintain the stability of the glow regime.[16] At atmospheric pressure, sub-mm gaps are required, which has led to the development of miniaturized dc GDs.[17,18] Although these devices have shown promise,[19] many remaining problems, particularly in the area of sample introduction, must be addressed in order to fully exploit their advantages. To avoid transient instabilities at the electrodes, radiofrequency (rf) powering schemes have also been used.[20] In some cases, the rf is combined with a dielectric barrier at the surface of at least one of the electrodes,[21–27] which usually leads to a plasma

Department of Chemistry, Indiana University, Bloomington, IN 47405, USA

composed of multiple filaments or streamers. Thus, the analytical use of such a dielectric barrier discharge (DBD), often termed an "atmospheric pressure glow discharge",[26,28] is limited by spatial and temporal inhomogeneities of the plasma. In any case, use of rf powering schemes results in the loss of some instrumental simplicity.

All these efforts, which reflect a strong interest in the operation of glow discharge sources at atmospheric pressure, have been guided by the common assumption that direct-current operation is restricted to reduced pressure. It has, however, long been known that, under certain conditions, the GAT can be avoided and stable and diffuse direct-current atmospheric-pressure glow discharges (dc APGD, or simply APGD) can be stably sustained.[14] Although atmospheric-pressure GDs using an electrolyte solution as one of the electrodes have been known for more than a century, they are beyond the scope of this work, which focuses on APGDs generated using metal electrodes.

APGDs were first reported by Thoma and Heer[29] and Fan,[30] who studied the transition between GDs and arcs. These authors showed that APGDs can be sustained in a variety of gases, including hydrogen and hydrogen–methane mixtures, oxygen, nitrogen and air. In the case of hydrogen, pressures up to 13 atmospheres could be applied before the transition to an arc was observed.[30] Gambling and Edels[31] extended the studies of the electrical characteristics of APGDs in air. Fan[30] suggested that factors other than thermionic emission should be used to explain the GAT. Thus, Boyle and Haworth[32] proposed a model based on field emission. In this model, arcing was attributed to field enhancements caused by irregularities in the surface of the electrodes. Rogoff[33] studied gas-heating effects in hydrogen APGDs and their relationship with the transition to an arc. Hieftje *et al.*[17,34] developed an atmospheric-pressure glow discharge generated in Ar that was termed a "microarc", and studied its application as a sample-introduction device. Mezei *et al.*[35,36] considered the deviation from similarity laws and the dependence of the positive-column cross section for dc helium and nitrogen glow discharges at several pressures, including atmospheric pressure. Arkhipenko *et al.*[37–44] performed extensive diagnostic studies on a He APGD, including the determination of the helium metastable concentrations within it, the decay kinetics of excited species in the presence of impurities, and several parameters associated with the cathode fall. Several studies described APGDs of different geometries in air and nitrogen.[45–51] Indeed, significantly more studies on APGDs have been performed in the last ten years than over the previous six decades. It is evident that there is considerable renewed interest in this subject.

In spite of this increased attention, few analytical applications of APGDs have appeared. Arkhipenko *et al.* proposed a high current ($\sim$1 ampere) APGD as source for elemental analysis,[37] although the results were not very encouraging. The most interesting application of an APGD was proposed more than a decade ago, when this source was used for the ionization of organic compounds.[52–54] In this approach, organic compounds were directly introduced into the discharge chamber of a low current ($\sim$1 mA) APGD sustained in helium.

One constraint that limits the application of APGDs is the lack of knowledge regarding their characteristics and operating conditions. Furthermore, the basic nature of an APGD, be it a real glow discharge or some form of stabilized arc, has been debated. For this reason, some effort in our laboratory during the last three years has been directed towards the characterization and analytical application of APGDs. The result of these studies has been an extremely versatile source that can be applied to the elemental analysis of solutions by optical spectroscopy[55] and mass spectrometry.[56] Additionally, the source can be employed for the ionization of organic compounds in the flowing afterglow mode.[57] The present study is devoted to the characterization of the He APGD. This manuscript will provide electrical and spectroscopic evidence which strongly suggests that the source is indeed a glow. It will also be shown that the transition from a conventional low-pressure GD to an APGD can be achieved without the formation of an arc.

Experimental

Reagents and instrumentation

High-purity He (99.999% ultra-high purity helium, Airgas, Radnor, PA) was used in all experiments.

The gas flow was set and monitored by means of a mass flow controller (Model FC-280-SAV, Tylan General, Carson, CA). The GD was operated with a direct-current high-voltage power supply (Model DRC-5-400R, Universal Voltronics, Mount Kisco, NY). Negative voltage was supplied to the cathode through a 2.5 kΩ ballast resistor placed in series. The anode was grounded. The source was always operated in current-controlled mode. The voltage was monitored before and after the ballast resistors by a high-voltage probe (Model P6013A, Tektronix Inc., Richardson, TX), which served also to calibrate the current displayed by the power supply.

A rotary vacuum pump (Model RV12, BOC-Edwards, Wilmington, MA) was used for the low-pressure studies. The pressure was monitored with a capacitance manometer (Baratron, MKS Instruments Inc., Wilmington, MA) in the low-pressure range (1–112 Torr) and with a mechanical vacuum gauge in the higher-pressure end (100 Torr to atmospheric pressure). In order to check for possible leaks, a 325 Moducell pressure gauge (HPS division, MKS Instruments Inc., Boulder, CO) operated with a 937 gauge controller (HPS division, MKS Instruments Inc., Wilmington, MA) working in the leak testing mode was connected to the GD cell. Leaks were tested by blowing helium outside the GD cell while the changes in pressure were monitored by the 937 gauge controller. The absence of leaks using this test was considered sufficient for this work.

Electrical and spectroscopic characterization. A 10-cm cubic aluminium cell was used as a discharge chamber for spectroscopic and electrical studies. The cell has suitable openings for vacuum, gas input and pressure monitoring, as shown in Fig. 1A. The anode and cathode were located on opposite faces of the cell. A side view of the discharge was possible by means of a quartz window. All openings were sealed with Viton® O-rings. When vacuum was not required, the vacuum line

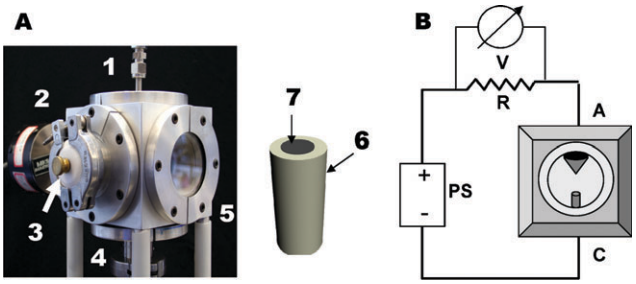

Fig. 1 GD cell used for electrical and spectroscopic studies and powering scheme. (A) Photograph of the cell and details of the cathode: (1) He line; (2) manometer; (3) cathode connector (the anode is on the opposite side, not seen in the photo); (4) vacuum line; (5) viewing window; (6) alumina shielding for the cathode; (7) tungsten rod (cathode). (B) Diagram of the system for powering the GD: PS, power supply; R, ballast resistor; V, voltmeter; C, cathode; A, anode.

was removed and replaced by a plate fitted with a 10 cm long 0.38 mm id gas exit tube.

The cathode was fabricated from a 3.0-mm diameter tungsten (>99.5% purity) rod with a flat, polished end. The cathode surface was polished with polishing paper of increasingly smaller grain size. The last stage of the polishing was performed using a 4/0 grit emery polishing paper (The Carborundum Company, Niagara Falls, New York), which yields a smooth and shiny surface, free of visible irregularities. The surface was then rinsed, first with water and then with methanol to remove any remaining dust or grease. This stage is important because any roughness in the cathode surface may lead to distortions of the electrical field density, which favors the GAT. Re-polishing the surface of the cathode between experiments was not required. A 3-mm i.d. alumina tube (6.35 mm o.d.) surrounding the cathode served to limit the cathode area. The anode was a cylindrical 25-mm diameter brass rod with a conical end (half angle $\sim 60^{\circ}$). The shape of the anode was found to be important to stabilize the discharge in the high pressure (>100 Torr) regime, as will be discussed below. The cathode was held in a fixed support, and the anode was mounted in a threaded base to permit adjustment of the inter-electrode gap. This gap, between the cathode and the tip of the anode, was always maintained at 1.0 cm unless otherwise stated.

A Canon digital camera (Model Rebel XT, Japan) was used to photograph the discharge. Because the brightness of the discharge changes markedly with pressure, the settings of the camera had to be adjusted to avoid saturation.

Spectroscopic measurements were performed by mounting the APGD in place of the inductively coupled plasma (ICP) ordinarily used in a commercial ICP emission spectrometer (ACTIVA, Horiba–Jobin Yvon, Longjumeau, France). The APGD was mounted on a movable support to allow its position to be adjusted. The spectral resolution with this instrument is between 8 pm (λ < 430 nm) and 16 pm (λ > 430 nm). The ACTIVA spectrometer provides simultaneous wavelength detection within a chosen spectral window (from approximately 10 nm in the low wavelength range to 3 nm at the visible end of the spectrum). Also, by the addition of a cylindrical lens between the front mirror and the entrance slit, improved spatial resolution in the vertical direction was achieved. Spatial resolution of approximately 0.2 mm (2.5 line pairs separated at 50%, 1951 USAF target, group 1–3) was obtained for images of up to 20 mm in size. Therefore, the entire inter-electrode gap could be simultaneously imaged.

Procedure

Electrical characteristics. At the beginning of all experiments the cell was evacuated (with no helium flowing) until the pressure reached a value below 0.3 Torr, the lowest pressure attainable with the roughing pump employed. Under these conditions no leaks were detected. The helium flow through the cell was then adjusted to 0.8 l min^{-1} and the pressure was regulated by means of a valve located in the vacuum line. Electrical characteristics of the GD were measured as a function of pressure. In particular, current was measured as a function of voltage (at constant pressure) and voltage was determined as a function of pressure (at constant current). Because of the considerably higher voltages required at low pressures, lower currents were used in order to avoid damage to the electrodes. In contrast, higher currents were used in the high-pressure range, as will be explained below.

Photographs were taken to illustrate the changes in discharge features that were observed at different pressures. It should be mentioned that the observed colors (described in the text) did not correspond exactly with those shown in later figures, probably because of differences between the effective discharge temperature and the color temperature of the CCD in the camera. Additionally, because of the limited dynamic range of commercial cameras and the marked range in intensity of the regions of the GDs, it is difficult to avoid saturation. Therefore, these photographs have only illustrative value.

Spectroscopic studies. For spectroscopic studies, the vacuum line was disabled and the cell was positioned in the ACTIVA ICP compartment. The electrodes were aligned with the ICP torch axis, so the entire inter-electrode gap was focused onto the entrance slit of the spectrometer. First, UV–visible spectra were collected over the range 160–800 nm with no spatial discrimination at different integration times in order to verify the absence of saturation effects. Then, emission maps of selected spectral regions were generated.

Rotational temperature profiles were estimated from emission maps of the Q1-branch of the OH emission[58] (excitation energies and transition probabilities were taken from ref. 58). Triplicate spectra were used. Boltzmann plots were linearized and the slope was calculated by the least-squares method. Temperature values with more than 20% RSD or generated from regression lines with a correlation coefficient lower than 0.85 were discarded.

Results and discussion

The transition from a low-pressure GD to an APGD

Qualitative aspects. The evolution of a gas discharge in helium as the pressure is raised is illustrated by the photographs in Fig. 2. At low pressures (<2 Torr) the discharge is sustained at high voltages (above 1 kV) and very low currents

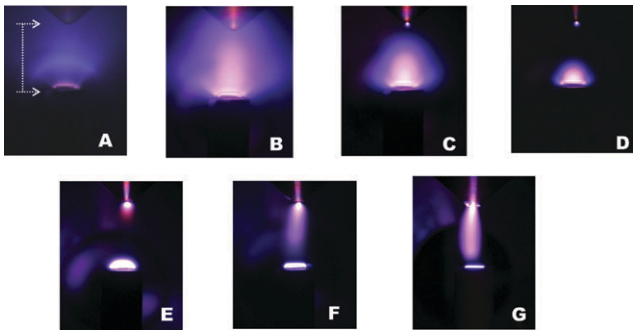

Fig. 2 GD at different pressures (top: anode, bottom: cathode, gap = 1 cm in all cases). (A) 1 Torr ($V = 1500$, $i \sim 200$ μA), the broken lines indicate the position of the electrodes; (B) 5 Torr ($V = 1500$ V, $i = 5$ mA); (C) 20 Torr ($V = 1200$ V, $i = 10$ mA); (D) 50 Torr ($V = 790$ V, $i = 25$ mA); (E) 95 Torr ($V = 570$ V, $i = 30$ mA); (F) 300 Torr ($V = 640$ V, $i = 30$ mA); (G) APGD ($V = 650$ V, $i = 30$ mA).

(below 1 mA) (Fig. 2A). The low degree of ionization under such conditions is evidenced by the presence of several alternating dark and bright ring-shaped regions around the cathode. When the pressure is increased to 5 Torr (Fig. 2B), however, the operating current rises to the mA range, and the applied voltage remains high (the discharge is operated in the current-controlled mode). Visually, the ring-shaped dark regions apparent in Fig. 2A shrink towards the surface of the cathode and the negative glow can now be seen as an intense reddish-pink sphere above the cathode. The positive column cannot be observed. As the pressure is raised incrementally to approximately 100 Torr (Fig. 2E) the easily observed negative glow declines in volume, which leaves a growing space between the negative glow and the anode (the positive column) that shows no emission (Fig. 2C–D). Only the anode glow is seen as a bright spot. During the transition between 80 and 100 Torr, a marked change in the characteristics of the discharge can be observed. In this case, the negative glow has become a thick disk at the cathode surface and a region of diffuse orange emission (possibly due to the He I 587.6 nm line) appears at the anode end of the positive column. This emission can be seen in Fig. 2E, which is seen as a faint reddish region close to the anode in the picture. As the pressure is raised from 100 to 760 Torr (Fig. 2E through 2G) most of the changes are observed in the positive column, while the negative glow evolves into a very thin bright layer on the surface of the cathode (Fig. 2F). The overall emission from the positive column grows significantly as a very diffuse cylinder having a diameter slightly larger than that of the cathode. Additionally, a bright pink–white emission plume in the positive column is observed to increase in intensity. At the anode surface itself, the positive column collapses into a single bright spot with a faint blue–violet emission around it. The maximum emission intensity of the positive column is located close to the anode. A very well defined dark region (*i.e.*, the Faraday dark space) separates the positive column from the negative glow (Fig. 2G).

Because the focus of the present study is on APGDs, it is appropriate to examine the structure of such a discharge in somewhat greater detail. The structure described above in connection with Fig. 2G is characteristic of a glow discharge

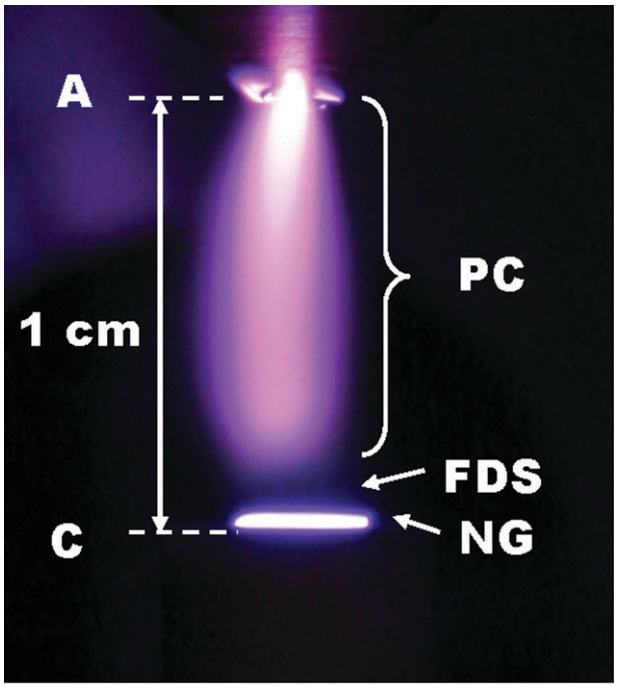

Fig. 3 Spatial structure of an APGD. Conditions are as in Fig. 2G. A: anode surface; C: cathode surface; PC: positive column; FDS: Faraday dark space; NG: negative glow (the horizontal asymmetry of the discharge is largely due to the direction of the gas flow).

at atmospheric pressure and is preserved throughout a wide range of currents and geometrical arrangements (*cf.* Fig. 3). The negative glow is always contained in a thin (sub-mm) layer close to the cathode surface and a large positive column fills the majority of the gap between the electrodes. This positive column is diffuse and, depending on the inter-electrode gap, has a diameter that can be significantly larger than that of the cathode. Because the positive column anchors to the anode at a single spot, a cone-shaped anode was used here to prevent fouling the discharge at high pressures. This contraction of the positive column at the anode end, however, must not be confused with the constriction of the positive column[33] that is characteristic of the GAT transition. The latter phenomenon generates a positive column having a very thin filamentary structure, and is usually accompanied by a marked increase in electrical conductivity of the discharge. The He APGD did not, at any time, show signs of becoming filamentary.

A variety of geometrical arrangements can sustain an APGD, and the one used in the present study was chosen for simplicity. In the system in Fig. 1A, the cathode area is limited by the alumina insulator and, as such, is always completely covered by the discharge. As a result, any changes in the observed current are intrinsically changes in the current density. With this system gaps up to 4 cm could be employed. Alternative cell designs having gaps up to 12 cm were also tested without compromising the discharge characteristics and stability. Importantly, even at atmospheric pressure the discharge maintains a diffuse and extremely stable structure. Additionally, the helium APGD can be operated for several hours without showing significant changes in the glow or degrading the electrode surfaces. No appreciable erosion or

damage of the electrodes can be observed, even after lengthy periods of operation ($\sim$100 hours), which is likely the result of the low sputtering capacity of He.

Electrical characteristics during the transition from a low-pressure GD to an APGD. The voltage stability was evaluated in each experiment by means of oscilloscope readings and Fourier power spectra. Discrete frequencies other than 60 Hz (<1%) were not detected. At high pressures (300–760 Torr) replicates of some experiments yielded a very reproducible current–voltage pattern, but shifted by a constant voltage (usually less than 50 V). This shift was attributed to slight differences in the anchoring point of the anode glow, but was not considered relevant for the purposes of this work. Although the discharge might anchor to slightly different points from one experiment to another, it remains fixed at the same point once the anode spot has been established.

Fig. 4 shows current–voltage curves (*V versus i*) for the GD operated at different ambient pressures. From the positive slopes of the *V–i* curves obtained at low pressure (Fig. 4A), it is clear that the GD is operating in the abnormal mode, which is consistent with the visual observation of a cathode completely covered by the discharge. In addition, the slope of this curve drops as the pressure is increased (see inset in Fig. 4A), which is in agreement with what has been already reported for other reduced-pressure glow discharges.[16,59] The lower dynamic resistance at higher pressures displayed in Fig. 4A can be attributed in part to an increase in the number of ionizing collisions produced by electrons when the density of the medium is higher. However, the GD undergoes a complex series of changes as the pressure is increased, which involve the change in the electron mean free path, electron number density and energy distribution function, ion electron recombination rate, *etc*. Because these physical changes are still under study, it is not possible to give, at this moment, a detailed account of the underlying processes.

The electrical behavior markedly changes at higher pressures, however (Fig. 4B). At pressures between 100 and 250 (not shown) Torr the voltage climbs as the current is raised from 10 to approximately 30 mA, until a maximum voltage of approximately 650 V is reached. Subsequent increases in the operating current do not yield as large a change in voltage. At higher pressures (from 300 Torr up to atmospheric pressure) the voltage is nearly independent of pressure for currents above 50 mA. The dominant pattern in this pressure range is that the slope of the current–voltage curves in the low-current region becomes lower as the pressure goes up, because of the higher voltages required to sustain the discharge in the low-current range.

The influence of pressure can be seen more clearly in Fig. 5, where the voltage required for sustaining the discharge is plotted as function of pressure while a constant current is maintained. Two well defined regions can be seen in this plot. At low pressures (<100 Torr), the voltage drops markedly as the pressure is raised. In this pressure regime, electrons require progressively less voltage to produce a given number of ionizing collisions as gas density goes up, because their mean-free path becomes smaller and losses to the walls of the discharge cell are reduced. At pressures around 100 Torr, however, the trend is reversed: a minimum voltage is reached, and the required discharge voltage increases with pressure. This trend at higher pressures can be explained by the necessity of overcoming the greater collisional frequency (*i.e*., reduction of the electrons' mean free path) by applying higher voltages. In other words, as the pressure is raised the amount of energy that the electrons can gain from a constant field is lessened. Thus, the ionization efficiency drops, and higher voltages are required to sustain the discharge. It is interesting that region A on the left side of Fig. 5 (where voltage drops as the pressure goes up) is coincident with the observed reduction of the volume of the negative glow. Additionally, the inflection point of this plot (see section B in Fig. 5) corresponds to the appearance of emission at the anode end of the positive column.

The rate of growth of the voltage with pressure in the medium to high pressure range (100–760 Torr) of Fig. 5 is inversely related to the discharge current. For low currents (<20 mA) a marked increase in the voltage as a function of pressure is observed, while for currents above 60 mA the voltage (*ca*. 650 V) is nearly independent of pressure over a

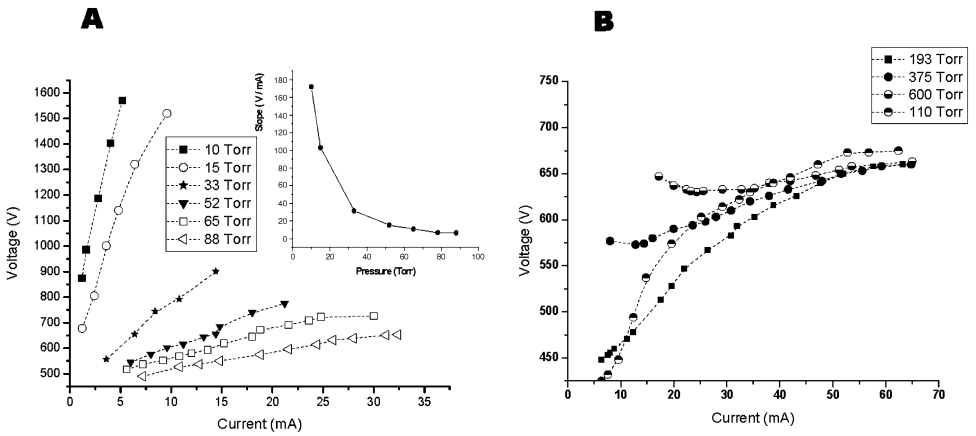

Fig. 4 Current–voltage curves for the GD operated at different pressures (gap = 1 cm). (A) Low-pressure range. The inset plot shows the slopes of the current–voltage curves as a function of pressure. (B) High-pressure range. The scale in this case has been expanded to more clearly show the observed changes. As the pressure increases, the behavior at the lowest current setting shows a trend towards negative resistance.

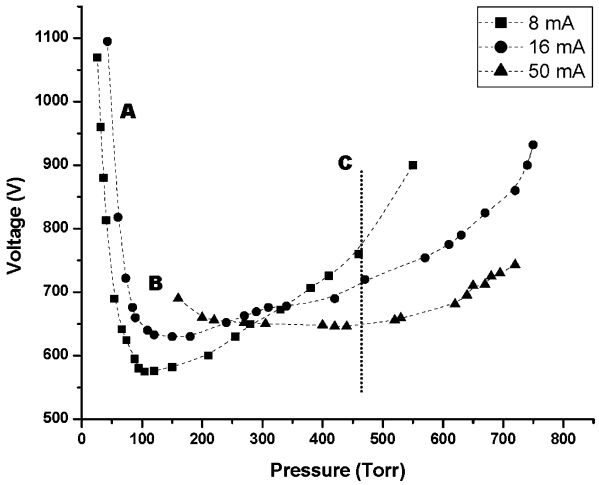

Fig. 5 Effect of ambient pressure on discharge voltage at different currents. Gap = 1 cm. (A) Region where shrinking of the negative glow is observed; (B) region where emission from the positive column appears; (C) the vertical line illustrates that, at a certain point, the discharge requires higher voltages to sustain lower currents.

wide range. We have also found that there is a threshold value (~950 V under the present experimental conditions) above which the discharge becomes unstable and forms an arc. Moreover, the higher the slope of the voltage *versus* pressure plots, the lower the pressure at which the system becomes unstable. For this reason, the GD could not be sustained at atmospheric pressure at currents below 20 mA in this system. Accordingly, plots such as those in Figs. 4 and 5 are useful to identify stability windows, *i.e.*, conditions where the GDs can be sustained in a high-pressure regime. These stability windows are, not surprisingly, strongly dependent on the system geometry, and particularly on the inter-electrode gap. The smaller the gap, the broader the stability region becomes. For gaps of 5 mm, the system can be operated at atmospheric pressure with currents as low as 5 mA. Additionally, the ballast resistor plays a significant role in maintaining a stable discharge. The larger the ballast resistor, the broader the range of operating conditions (gaps, currents) where the discharge is stable. By doubling the value of the ballast resistor we found that the discharge could be operated stably at 20 mA.

These results illustrate that it is possible to change from a conventional low-pressure He GD to an APGD without abrupt changes in the electrical properties. Thus, it is clearly demonstrated that the APGD is not an isolated phenomenon attributable to specific, unconventional, and difficult-to-reproduce instrumental conditions or geometries. A dc diffuse discharge in He can be sustained over a broad pressure range, and the He APGD evolves in a continuous fashion from traditional low-pressure GDs. In the following sections the electrical and spectroscopic characteristics of this new APGD will be examined in greater detail.

Helium APGD: glow or arc?

Electrical characteristics. The electrical behavior of a gas discharge is often used as a way of classifying its working regime. When the GD voltage is independent of the operating current, the discharge is considered to be operating in the normal mode, whereas if the voltage rises with current the GD is viewed as operating in abnormal mode.[1,14,16] In terms of these definitions, APGDs exhibit unique behavior. Above a certain pressure (see point C in Fig. 5), GDs have a negative dynamic resistance, *i.e.*, lower voltages are required to sustain higher currents. Fig. 6A shows this behavior in more detail for an APGD with different inter-electrode gaps. The slopes of these current–voltage curves become more negative as the gap is increased. The negative dynamic resistance of APGDs is well known,[14,15,35,60] and for this reason a ballast resistor is required. The ballast resistor serves to limit the power supplied to the discharge, thereby avoiding arcing. Therefore, a larger ballast resistor (5 kΩ) was used to evaluate larger gaps in Fig. 6A. In Fig. 6B, the linear effect of the inter-electrode gap on the discharge voltage is shown explicitly. With the cell described in this work, gaps up to 4 cm could be employed. However, preliminary experiments with an alternative cell design permitted generation of a stable discharge with gaps of up to 12 cm, provided a sufficiently large ballast resistor (capable of compensating for the negative dynamic resistance of the APGD) was used.

Although the previous section demonstrated that it is possible to change from a low-pressure to an atmospheric-pressure GD in a smooth fashion, the question remains whether the APGD can actually be considered a glow, or

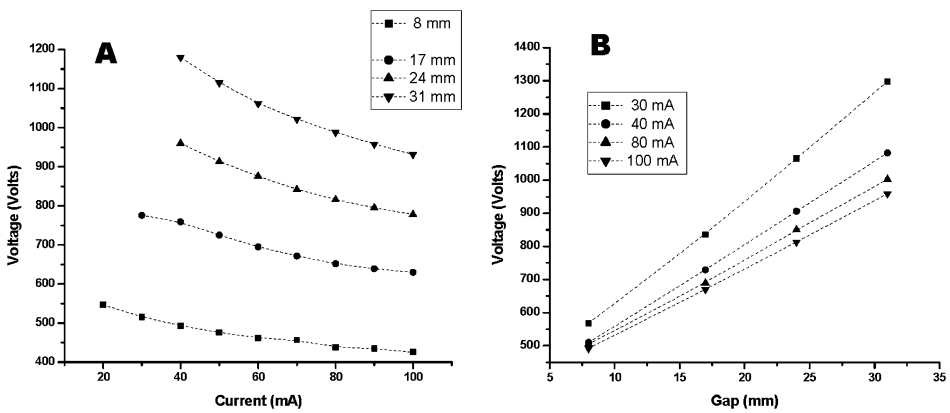

Fig. 6 Electrical characteristics of the He APGD. (A) Current–voltage curves for different inter-electrode gaps. (B) Effect of inter-electrode gap on operating voltage for different discharge currents. 5 kΩ ballast resistor used.

whether it is just a specialized form of an arc. Given the marked differences between the two regimes, this question is relevant from both an analytical and theoretical point of view. The electrical characteristics of the APGD strongly suggest that this discharge is, in fact, not operating as an arc. First, arcs function at lower voltages (usually less than 100 V).[14–16] Second, the transition from a glow discharge to an arc is clearly seen as a marked drop in the operating voltage of the discharge,[30,31] which has not been observed in the present experiments. Third, arcs run with current densities of at least 100 A cm^{-2}, while in the current experiments the maximum cathodic current density was 1.4 A cm^{-2} (for a 100 mA current). Although it is true that the anodic current density is considerably higher, this discharge never became filamentary, even when large gaps were tested. Such behavior was maintained even at the highest currents (100 mA) investigated here. Literature suggests that this "glow" regime may, in fact, be sustained for currents up to several amperes.[39]

Spectroscopic characteristics of a He APGD

Although the information described previously is relevant to the operation of an APGD, the ultimate goal of an analytical plasma source is to produce an efficient transfer of energy from the electrical field to the electrons and the buffer gas, which can then be utilized for the ionization and excitation of analyte species. For this reason, spectroscopic characterization is essential to determine the utility of the plasma as an analytical source.

Fig. 7 shows a UV–visible spectrum of the APGD used in this study. Apart from the He lines, emission from several impurities (trace amounts of N_2, H_2O, O_2) can be observed. In spite of the high-purity helium used and several attempts to purify the gas on-line (drying, traps, *etc.*), emission from these species was always present. Difficulties associated with the purity of the gas in He-based discharges are well known,[61] because the high ionization/excitation efficiency of these plasmas allows impurities to be detected at very low levels. Removing these impurities often requires extensive cleaning and baking of the gas lines and special purification strategies

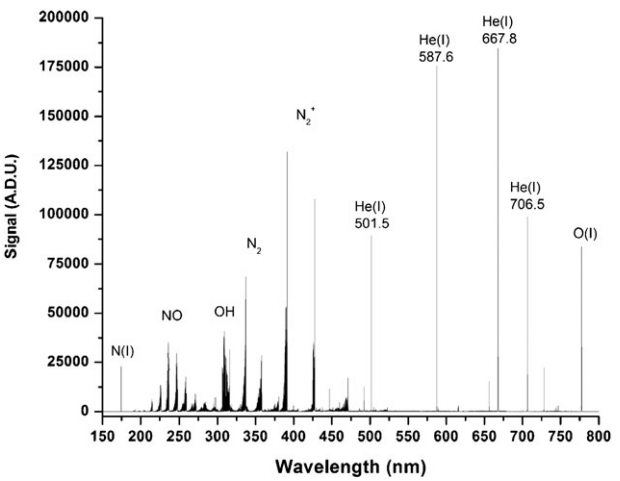

Fig. 7 UV–vis emission spectrum of the He APGD. The number on the main He lines corresponds to the wavelength (in nm).

(such as cataphoretic purifiers). These heroic measures were not considered necessary for the present work.

Apart from the He I lines, the most intense emission from the discharge is attributable to N_2^+ (band heads at 391.4 nm and 427 nm). Characteristic emission from N I (lines at 174.3 and 174.5 nm), N_2 (band heads at 337 and 380 nm), OH (band heads at 281 and 306 nm), NO (γ system with double-headed bands below 300 nm) and O I (triplet at 777.2, 777.4 and 777.5 nm) was also observed. The ability to detect these impurities, particularly in the positive column, was greatly improved by the extremely low background levels observed in the emission spectrum. Importantly, emission from the cathode material (W) was not detected, probably because of the low sputtering efficiency of He.

The spatial distribution of selected emission features is shown in Figs. 8 and 9. All the He lines that were studied (501.5 nm, 587.6 nm, 667.8 nm and 706.5 nm) have a similar pattern (Fig. 8A): the emission is very intense in regions close to the electrodes, and it is stronger at the cathode than at the anode. It is also found that the increase of emission with current is more pronounced at the anode than at the cathode. Emission from the nitrogen molecular ion (N_2^+) has a pattern similar to that of He lines (Fig. 8B). This similarity might be related to the mechanism of production of this ion. There is widespread agreement[26,62,63] that N_2^+ is formed in helium discharges through both Penning ionization (1) and charge transfer (2), both of which involve helium:

$$He^* + N_2 \rightarrow He + N_2^+ + e \quad (1)$$

$$He_2^+ + N_2 \rightarrow 2\,He + N_2^+ \quad (2)$$

(where He* represents one of the metastable states of helium). The N_2^+ ion is initially formed in an excited state and upon decay, the characteristic emission of the first negative system (band head at 391.4 nm) can be seen. For this reason, the emission of N_2^+ has been used as a way of detecting the presence of both He_2^+ and He*.[64,65] Although it is not possible to determine *a priori* which of these reactions (1 or 2) will be dominant, it is evident that some species in the regions close to the electrodes have enough energy to efficiently ionize and excite N_2, the ionization potential of which is 15.6 eV. In Fig. 8B (see inset plot) the spatial distribution of atomic nitrogen is shown. It has been reported[66] that N_2^+ can be quickly destroyed by dissociative recombination:

$$N_2^+ + e^- \rightarrow N + N^* \quad (3)$$

(where N* is a nitrogen atom in an excited state); because of the high rate constant of this reaction, this might be—at least in part—the source of atomic nitrogen.

Unlike the profiles in Fig. 8, the emission from some molecular species (N_2, NO) is particularly intense in the positive column (Fig. 9). For N_2, the emission close to the electrodes is always higher than in the positive column. Interestingly, the emission in the anode region becomes considerably stronger than that in the negative glow as the current is raised (Fig. 9A). The emission from NO, on the other hand, is always higher in the positive column and, unlike any other profile, the emission in the negative glow drops as current is

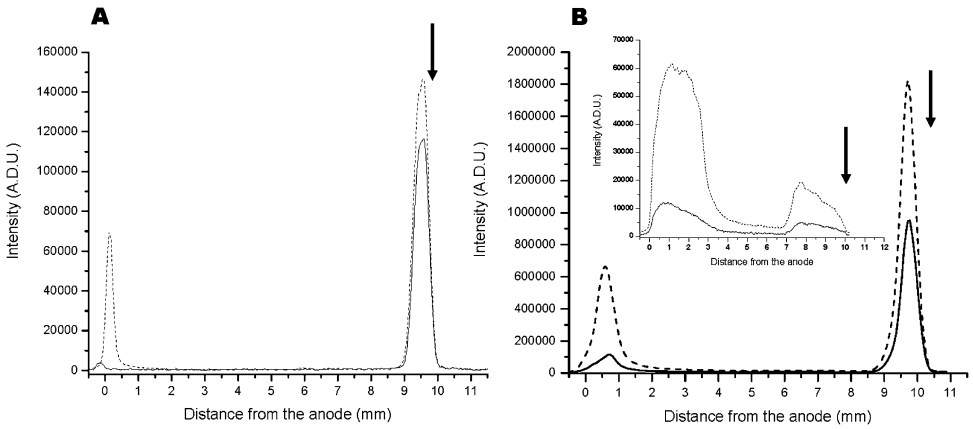

Fig. 8 Emission maps of several species in the He APGD at different discharge currents. (A) He I (706.5 nm); (B) N_2^+ (391.4 nm). The inset plot shows the spatial distribution of N I (174.5 nm) emission. The arrow indicates the position of the cathode. Discharge current = 30 mA (solid line) and 50 mA (broken line).

increased (Fig. 9B). This drop might be due to dissociation of NO at higher currents.

Emission maps of OH can be seen in Fig. 10A. These profiles are similar to those found for nitrogen in Fig. 9, with significant emission in the positive column and particularly strong emission in the vicinity of the electrodes. Also, as the current grows, the emission near the anode becomes prominent. From these emission maps, rotational-temperature profiles were calculated (Fig. 10B). The temperature in the region close to the cathode (approximately 1 mm from the surface of the electrode) could not be estimated within acceptable limits for the error. This large error might be a result of the high temperature gradient in this region and the limited spatial resolution (in the fractional mm range). Temperatures in the positive column range from approximately 1300 K at 30 mA to 1500–1800 K at 50 mA. Temperatures tend to rise towards the anode, a trend that is more pronounced at higher currents.

One of the most important aspects of the maps in Figs. 8–10 is the clear evidence of a well-defined spatial structure in the discharge, which reflects the precise gradients of electrical potential that are generated between the electrodes.[26] This precise distribution of electrical fields is, in fact, a distinctive feature of GDs.[16] Unlike other gas discharges, GD can "hold" large electrical potentials between the electrodes due to the generation of a space-charge structure in the vicinity of the cathode.[16] Thus, electrons can gain a large amount of energy in the region close to the cathode, but they are slowed down as they move farther away from it. This structure prevents an ionizing cascade that would lead to an arc. Because of this process, electrical energy can be transmitted to the buffer gas from the electrons in a non-thermal fashion in particular regions of the discharge. The dark space separating the two strongly emitting regions (*i.e.*, the negative glow and positive column) is evidence of the non-thermal nature of this source. Such spectroscopic evidence adds support to the idea that the APGD is effectively a glow. As a distinct feature of APGD sources, however, emission from the anode end of the positive column is qualitatively similar to the emission in the cathodic region.

The foregoing evidence proves that it is possible to sustain a discharge with a glow-like structure at atmospheric pressure. Unfortunately, quantitative models for high-pressure (100–760 Torr) dc GDs have not yet been developed. Therefore it is difficult to provide a detailed explanation for the results shown above. Apparently, at higher pressures, diffusional losses (losses to the walls and the electrodes) become less important,[67] while recombination should be the dominant mechanism for charge loss. Several studies have shown that

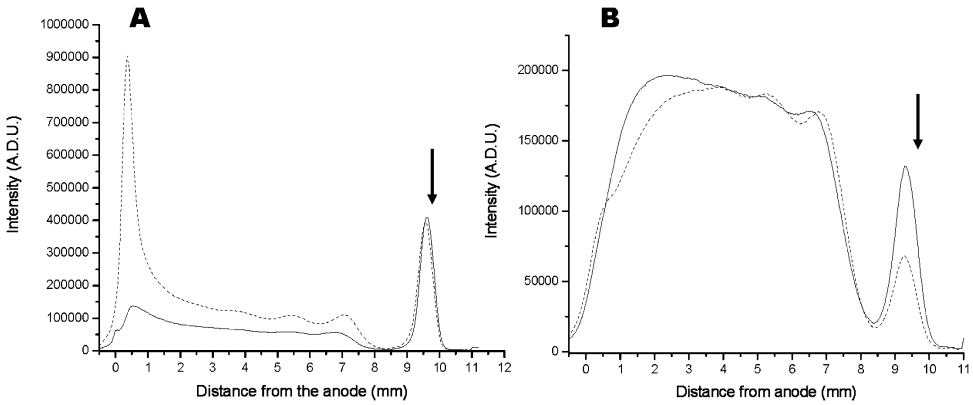

Fig. 9 Emission maps of molecular species in the He APGD at different discharge currents. (A) N_2 (337 nm); (B) NO (237 nm). The arrow indicates the position of the cathode. Discharge current = 30 mA (solid line) and 50 mA (broken line).

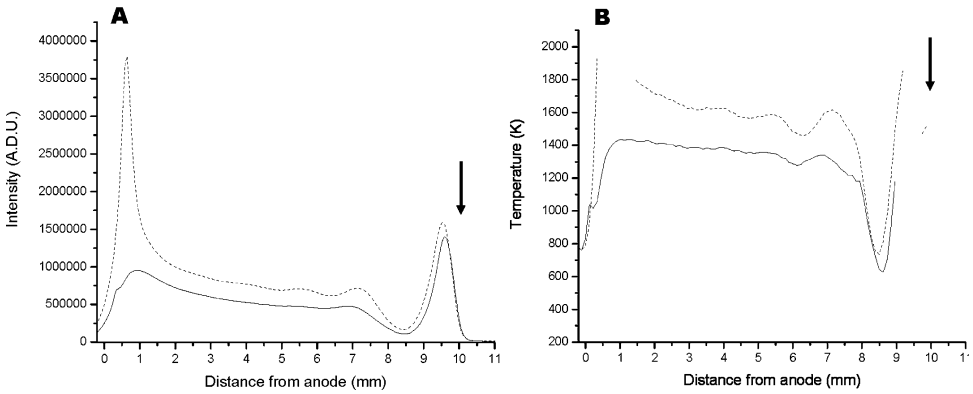

Fig. 10 OH emission maps and rotational temperatures in the He APGD at different discharge currents. (A) OH emission (306 nm); (B) calculated rotational temperature. The arrow indicates the position of the cathode. Discharge current = 30 mA (solid line) and 50 mA (broken line).

He_2^+ becomes a dominant species as the pressure is increased in a GD,[67–69] and it has also been estimated that the same ion should be the main source of helium metastables in the afterglow of a He discharge at atmospheric pressure.[70] Owing to the nature and structure of the APGD, the positive column should have a substantial influence on the overall behavior of the discharge. Several studies have shown that, under certain operating conditions, the positive columns of low- and medium-pressure GDs show a negative dynamic resistance.[15,60,71,72] This effect is particularly present at low currents, and has a significant impact on the properties of the whole GD.

There is a wide range of analytical applications where this new glow discharge can be used. The OH rotational temperature, which can be used as an approximation of the gas kinetic temperature, is relatively high when compared with low pressure devices. It is well known[14] that an increase in the pressure of the GD usually leads to a higher gas kinetic temperature. Despite the reduction in the electron mean free path, which reduces the energy gained by the electrons between collisions, the higher collisional frequency results in a more efficient transfer of energy to the gas. These trends are evident from the results reported by Dothan and Kagan,[68] who studied a low pressure glow discharge in helium. In this work, the gas temperaure increased with pressure and, for the highest pressure studied (40 Torr), the temperature reached 440 K at 40 mA. The profiles shown in Fig. 10 reveal that for a similar current the He APGD has a significantly higher gas temperature. In general, the temperature ranges from 1300 to 1600 K in the positive column, and it is slightly higher at the surface of the electrodes. These temperatures are lower than those reported for other types of atmospheric pressure glow discharges, such as those using an electrolyte solution as the cathode.[73,74] However, they are promising because they allow, for example, droplet desolvation, which is difficult to achieve in a low pressure GD. In fact, we have recently reported the use of a He APGD for the elemental analysis of solutions by atomic emission spectrometry,[55] and hydride generation-mass spectrometry[56] using a He APGD has been recently published. As with the low pressure counterparts, the use of the He APGD can also be extended to the analysis of organic compounds.[57] In any case, further investigation is required in order to characterize this novel plasma source and fully exploit its analytical applications.

Conclusions

This study has shown that it is possible to sustain a glow-like discharge over a wide range of pressures, even at atmospheric pressure. The electrical and spectroscopic results strongly suggest that the source is under a glow regime. The He APGD shows an outstanding stability and extremely simple instrumental setup. A preliminary characterization shows promise regarding the application of this device with analytical purposes. Further studies are still required in order to fully exploit its analytical applications and to elucidate the mechanisms involved.

Acknowledgements

Support for this work was provided by the U.S. Department of Energy (grant number DE-FG02-98ER 14890), Office of Nonproliferation Research and Engineering. The authors thank Indiana University Mechanical Instrument Services, LECO Corporation and Jobin-Yvon–Horiba for their support.

References

1 R. K. Marcus and J. A. C. Broekaert, *Glow Discharge Plasmas in Analytical Spectroscopy*, John Wiley, Chichester, 2003.
2 S. A. McLuckey, G. L. Glish, K. G. Asano and B. C. Grant, *Anal. Chem.*, 1988, **60**, 2220–2227.
3 T. M. Brewer, J. Castro and R. K. Marcus, *Spectrochim. Acta, Part B*, 2006, **61**, 134–149.
4 V. Majidi, M. Moser, C. Lewis, W. Hang and F. L. King, *J. Anal. At. Spectrom.*, 2000, **15**, 19–25.
5 C. L. Lewis, M. A. Moser, W. Hang, D. E. Dale, Jr, D. C. Hassell and V. Majidi, *J. Anal. At. Spectrom.*, 2003, **18**, 629–636.
6 C. L. Lewis, M. A. Moser, D. E. Dale, Jr, W. Hang, C. Hassell, F. L. King and V. Majidi, *Anal. Chem.*, 2003, **75**, 1983–1996.
7 J. P. Guzowski, Jr and G. M. Hieftje, *J. Anal. At. Spectrom.*, 2000, **15**, 27–36.
8 R. Mason and D. Milton, *Int. J. Mass Spectrom. Ion Processes*, 1989, **91**, 209–225.

9 K. Newman and R. S. Mason, *J. Anal. At. Spectrom.*, 2004, **19**, 1134–1140.
10 R. K. Marcus, E. H. Evans and J. A. Caruso, *J. Anal. At. Spectrom.*, 2000, **15**, 1–5.
11 K. Newman and R. S. Mason, *J. Anal. At. Spectrom.*, 2005, **20**, 830–838.
12 R. E. Steiner, C. L. Lewis and V. Majidi, *J. Anal. At. Spectrom.*, 1999, **14**, 1537–1541.
13 H. Conrads and M. Schmidt, *Plasma Sources Sci. Technol.*, 2000, **9**, 441–454.
14 A. M. Howatson, *An Introduction to Gas Discharges*, Pergamon Press, New York, 2nd edn., 1976.
15 E. E. Kunhardt and L. H. Luessen, *NATO Advanced Science Institute Series, Series B, Physics, Vol. 89: Electrical Breakdown and Discharge in Gases, Pt. B: Macroscopic Processes and Discharges*, 1983.
16 Y. P. Raizer, *Gas Discharge Physics*, Springer, Berlin, 1992.
17 L. R. Layman and G. M. Hieftje, *Anal. Chem.*, 1975, **47**, 194–202.
18 J. Franzke, K. Kunze, M. Miclea and K. Niemax, *J. Anal. At. Spectrom.*, 2003, **18**, 802–807.
19 V. Karanassios, *Spectrochim. Acta, Part B*, 2004, **59**, 909–928.
20 R. Guevremont and R. E. Sturgeon, *J. Anal. At. Spectrom.*, 2000, **15**, 37–42.
21 S. Kanazawa, M. Kogoma, T. Moriwaki and S. Okazaki, *J. Phys. D: Appl. Phys.*, 1988, **21**, 838–840.
22 T. Yokoyama, M. Kogoma, T. Moriwaki and S. Okazaki, *J. Phys. D: Appl. Phys.*, 1990, **23**, 1125–1128.
23 S. Okazaki, M. Kogoma, M. Uehara and Y. Kimura, *J. Phys. D: Appl. Phys.*, 1993, **26**, 889–892.
24 M. Stefecka, D. Korzec, M. Siry, Y. Imahori and M. Kando, *Sci. Technol. Adv. Mater.*, 2001, **2**, 587–593.
25 L. Mangolini, K. Orlov, U. Kortshagen, J. Heberlein and U. Kogelschatz, *Appl. Phys. Lett.*, 2002, **80**, 1722–1724.
26 C. Anderson, M. Hur, P. Zhang, L. Mangolini and U. Kortshagen, *J. Appl. Phys.*, 2004, **96**, 1835–1839.
27 L. Mangolini, C. Anderson, J. Heberlein and U. Kortshagen, *J. Phys. D: Appl. Phys.*, 2004, **37**, 1021–1030.
28 G. Nersisyan, T. Morrow and W. G. Graham, *Appl. Phys. Lett.*, 2004, **85**, 1487–1489.
29 H. Thoma and L. Heer, *Z. Tech. Phys.*, 1932, **13**, 464–470.
30 H. Y. Fan, *Phys. Rev.*, 1939, **55**, 769–775.
31 W. A. a. E. Gambling and H., *Br. J. Appl. Phys.*, 1954, **5**, 36–39.
32 W. S. Boyle and F. E. Haworth, *Phys. Rev.*, 1956, **101**, 935–938.
33 G. I. Rogoff, *Phys. Fluids*, 1972, **15**, 1931–1940.
34 R. I. Bystroff, L. R. Layman and G. M. Hieftje, *Appl. Spectrosc.*, 1979, **33**, 230–240.
35 P. Mezei, T. Cserfalvi, M. Janossy, K. Szocs and H. J. Kim, *J. Phys. D: Appl. Phys.*, 1998, **31**, 2818–2825.
36 P. Mezei, T. Cserfalvi and M. Janossy, *J. Phys. D: Appl. Phys.*, 2001, **34**, 1914–1918.
37 V. I. Arkhipenko, S. M. Zgirovskii, A. K. Kapanik, L. V. Simonchik and D. A. Solov'yanchik, *J. Appl. Spectrosc.*, 1998, **64**, 721–725.
38 V. I. Arkhipenko, S. M. Zgirovskii and L. V. Simonchik, *J. Appl. Spectrosc.*, 1999, **66**, 386–393.
39 V. I. Arkhipenko, S. M. Zgirovskii, N. Konjevic, M. M. Kuraica and L. V. Simonchik, *J. Appl. Spectrosc.*, 2000, **67**, 910–918.
40 V. I. Arkhipenko, S. M. Zgirovskii and L. V. Simonchik, *J. Appl. Spectrosc.*, 2000, **67**, 731–736.
41 V. I. Arkhipenko, S. M. Zgirovskii, A. A. Kirillov and L. V. Simonchik, *Plasma Phys. Rep. (Transl. of Fiz. Plazmy (Moscow))*, 2002, **28**, 858–865.
42 V. I. Arkhipenko, V. Z. Greben, V. A. Dlugunovich, S. M. Zgirovskii and L. V. Simonchik, *J. Appl. Spectrosc.*, 2004, **71**, 410–416.
43 V. I. Arkhipenko, S. M. Zgirovskii, A. A. Kirillov and L. V. Simonchik, *J. Appl. Spectrosc.*, 2005, **72**, 576–584.
44 V. I. Arkhipenko, A. A. Kirillov, L. V. Simonchik and S. M. Zgirouski, *Probl. At. Sci. Technol., Ser.: Plasma Phys.*, 2005, 199–201.
45 X. Duten, D. Packan, L. Yu, C. O. Laux and C. H. Kruger, *IEEE Trans. Plasma Sci.*, 2002, **30**, 178–179.
46 R. Morent and C. Leys, *Czech. J. Phys.*, 2004, **54**, 1068–1073.
47 A.-A. H. Mohamed, R. Block and K. H. Schoenbach, *IEEE Trans. Plasma Sci.*, 2002, **30**, 182–183.
48 O. Goossens, T. Callebaut, Y. Akishev, A. Napartovich, N. Trushkin and C. Leys, *IEEE Trans. Plasma Sci.*, 2002, **30**, 176–177.
49 D. Staack, B. Farouk, A. Gutsol and A. Fridman, *Plasma Sources Sci. Technol.*, 2005, **14**, 700–711.
50 R. H. Stark and K. H. Schoenbach, *Appl. Phys. Lett.*, 1999, **74**, 3770–3772.
51 R. H. Stark and K. H. Schoenbach, *J. Appl. Phys.*, 1999, **85**, 2075–2080.
52 I. Sofer, J. Zhu, H. S. Lee, W. Antos and D. M. Lubman, *Appl. Spectrosc.*, 1990, **44**, 1391–1398.
53 J. Zhao, J. Zhu and D. M. Lubman, *Anal. Chem.*, 1992, **64**, 1426–1433.
54 Y. B. Golubovskii, V. A. Maiorov, J. Behnke and J. F. Behnke, *J. Phys. D: Appl. Phys.*, 2003, **36**, 39–49.
55 M. R. Webb, F. J. Andrade and G. M. Hieftje, *Winter Conference on Plasma Spectrochemistry, Tucson, Arizona*, 2006.
56 W. C. Wetzel, F. J. Andrade, J. A. C. Broekaert and G. M. Hieftje, *J. Anal. At. Spectrom.*, 2006, **21**, 750–756.
57 F. J. Andrade, S. J. Ray, W. C. Wetzel, M. R. Webb, G. Gamez and G. M. Hieftje, *Proceedings of the 54th ASMS Conference in Mass Spectrometry and Allied Topics*, Seattle, WA, 2006.
58 R. S. Houk and Y. Zhai, *Spectrochim. Acta, Part B*, 2001, **56**, 1055–1067.
59 A. Bogaerts, PhD Thesis, Universiteit Antwerpen, Antwerp, 1996.
60 A. A. Yahya and J. E. Harry, *Int. J. Electron.*, 1999, **86**, 755–762.
61 M. C. Hunter, K. D. Bartle, A. C. Lewis, J. B. McQuaid, P. Myers, P. W. Seakins and C. Van Tilburg, *J. High Resolut. Chromatogr.*, 1998, **21**, 75–80.
62 C. Collins, W. W. Robertson, E. E. Ferguson and F. A. Matsen, *J. Am. Chem. Soc.*, 1962, **84**, 676.
63 F. Massines, A. Rabehi, P. Decomps, R. Ben Gadri, P. Segur and C. Mayoux, *J. Appl. Phys.*, 1998, **83**, 2950–2957.
64 C. B. Collins and W. W. Robertson, *Spectrochim. Acta, Part B*, 1963, **19**, 747–751.
65 C. B. Collins and W. W. Robertson, *J. Chem. Phys.*, 1964, **40**, 701–712.
66 M. J. van de Sande, P. van Eck, A. Sola, A. Gamero and J. J. A. M. van der Mullen, *Spectrochim. Acta, Part B*, 2003, **58**, 457–467.
67 K. Kutasi, P. Hartmann and Z. Donko, *J. Phys. D: Appl. Phys.*, 2001, **34**, 3368–3377.
68 F. Dothan and Y. M. Kagan, *J. Phys. D: Appl. Phys.*, 1979, **12**, 2155–2166.
69 Y. Ichikawa and S. Teii, *J. Phys. D: Appl. Phys.*, 1980, **13**, 2031–2043.
70 J. Stevefelt, J. M. Pouvesle and A. Bouchoule, *J. Chem. Phys.*, 1982, **76**, 4006–4015.
71 J. E. Lawler, *Phys. Rev. A*, 1980, **22**, 1025–1033.
72 J. E. Lawler and U. Kortshagen, *J. Phys. D: Appl. Phys.*, 1999, **32**, 3188–3198.
73 M. R. Webb, F. J. Andrade, G. Gamez, R. McCrindle and G. M. Hieftje, *J. Anal. At. Spectrom.*, 2005, **20**, 1218–1225.
74 W. C. Davis and R. K. Marcus, *Spectrochim. Acta, Part B*, 2002, **57B**, 1473–1486.

